

Influence of Internal Topologies on Components Produced by Selective Laser Melting: Numerical Analysis

C. Malça, P. Gonçalves, N. Alves, A. Mateus

Abstract—Regardless of the manufacturing process used, subtractive or additive, material, purpose and application, produced components are conventionally solid mass with more or less complex shape depending on the production technology selected. Aspects such as reducing the weight of components, associated with the low volume of material required and the almost non-existent material waste, speed and flexibility of production and, primarily, a high mechanical strength combined with high structural performance, are competitive advantages in any industrial sector, from automotive, molds, aviation, aerospace, construction, pharmaceuticals, medicine and more recently in human tissue engineering. Such features, properties and functionalities are attained in metal components produced using the additive technique of Rapid Prototyping from metal powders commonly known as Selective Laser Melting (SLM), with optimized internal topologies and varying densities. In order to produce components with high strength and high structural and functional performance, regardless of the type of application, three different internal topologies were developed and analyzed using numerical computational tools. The developed topologies were numerically submitted to mechanical compression and four point bending testing. Finite Element Analysis results demonstrate how different internal topologies can contribute to improve mechanical properties, even with a high degree of porosity relatively to fully dense components. Results are very promising not only from the point of view of mechanical resistance, but especially through the achievement of considerable variation in density without loss of structural and functional high performance.

Keywords—Additive Manufacturing, Internal topologies, Porosity, Rapid Prototyping, Selective Laser Melting.

I. INTRODUCTION

THE interest in additive techniques of Rapid Prototyping (RP) reached a considerable impetus in the last decade. The main motivation for the development of this technology stemmed from the industry needs in exploiting the advantages of these production processes in conjunction with the research

undertaken by the academic community in the search for technological advances and constant optimization of these processes. Compared to conventional subtractive techniques, additive techniques have the additional advantage of geometrical freedom of construction [1]-[3]. Among other additive RP techniques, Selective Laser Melting (SLM) offers a wide range of advantages in the production of prototypes or metallic components, e.g., lower time-to-market, high rate of use of materials, direct production from three-dimensional CAD model, high level of flexibility, i.e. products with different geometries can be produced in the same batch, flexibility of the material being processed, high flexibility in the selection of metallic materials to be used, high production rates, mass customization, versatility, precision, geometric freedom, and the ability to create unique designs with intrinsic characteristics of engineering [4]-[8].

SLM has been successfully applied using materials such as aluminum, copper, iron, stainless steel, chromium, nickel alloys, titanium and composites of these materials. However, it is unquestionable that the great advantage of SLM is associated with the production of components with high mechanical strength, from the generation and optimization of internal topologies consisting of thin-walled, hidden voids and channels. These topologies represent a considerable weight reduction without compromising stability, reliability and mechanical strength of the prototypes or components [5], [8]. In this respect, multiple internal topologies, with different degrees of porosity - due to the different orientations of the inner filaments -, were modeled and their mechanical behavior numerically evaluated through compression and bending testing. With this objective, a Finite Element Analysis (FEA) was performed, from the 3D CAD model of each developed topology, using a commercial finite element code. The internal topologies modeled in this work were essentially aimed at the production of components with a high degree of porosity compared to fully dense components, i.e. to meet a balance between the porosity of the component, not compromising its structural behavior, and maintaining the mechanical resistance for bending and compression.

II. NUMERICAL MODELING

To take advantage of the features of RP additive techniques, in particular SLM, test specimens with different internal topologies were developed to assess which kind of internal structures would present better mechanical behavior

C. Malça is with the Mechanical Engineering Department, Polytechnic Institute of Coimbra, R. Pedro Nunes, 3030-199 Coimbra, Portugal and with the Centre for Rapid and Sustainable Product Development, Polytechnic Institute of Leiria, Rua de Portugal, 2430-028 Marinha Grande, Portugal (e-mail: candida@isec.pt).

P. Gonçalves is with the Mechanical Engineering Department, Polytechnic Institute of Coimbra, R. Pedro Nunes, 3030-199 Coimbra, Portugal (e-mail: pedro84ndf@gmail.com).

N. Alves and A. Mateus are with the Centre for Rapid and Sustainable Product Development, Polytechnic Institute of Leiria, Rua de Portugal, 2430-028 Marinha Grande, Portugal (e-mail: nuno.alves@ipleiria.pt, artur.mateus@ipleiria.pt).

when subjected to a particular type of load under mechanical compression and bending tests. Based on the work presented by Domingos et al. [9], three alternative internal topologies were modeled using a 3D CAD commercial software. Topologies differ in the fillers orientation: fillers driven to zero and ninety degrees ($0^\circ/90^\circ$); $45^\circ/135^\circ$; and $60^\circ/120^\circ$. Figs. 1 (a)-(c) show the corresponding guidelines of fibers in each one of internal topology modeled.

To perform the mechanical testing of bending and compression, test specimens were coated by an external box with a thickness of 0.8 mm as shown in Figs. 2 (a)-(c). Figs. 3 (a)-(c) illustrate the cross section of test specimens modeled. It should be noted that the involving box has the main purpose of producing well defined test specimens, with well-defined dimensions and regular surfaces.

Figs. 4 (a) and (b) illustrate the boundary and load conditions applied to the 3D CAD model developed, in order to simulate the compression and bending mechanical tests, respectively.

In terms of load conditions, a load of 2.2 kN was applied for bending, whereas for compression tests a load of 25 kN was considered. Concerning boundary conditions, constraints of no displacements and rotations, i.e. rigidly fixed conditions, were applied at the regions marked in green in Fig. 4. With respect to material elastic properties, a CoCr alloy with a tensile strength of ca. 1050 MPa, a yield strength of approximately 850 MPa and a hardness of 35 RC was selected to perform FEA.

Next section presents FEA results obtained for external compression and bending loading of the test specimens numerically modeled with different internal geometries. Regardless of topology type, both Figs. 2 and 3 depict the relatively fine mesh of triangular elements applied. The selected solid mesh resulted from the meshing sensitivity study previously performed.

III. NUMERICAL RESULTS

Analysis using the finite element method provides insight into the stress concentrators' and displacements magnitude and location. Areas of greatest magnitudes are shown in red. Figs. 5 and 6 illustrate the stress gradients obtained for the bending and compression mechanical tests, respectively. Concerning bending tests, Figs. 5 (a)-(c) show that there are no considerable changes worthy of note. However, it should be noted that the topology $0^\circ/90^\circ$ led to the lowest value of the maximum stress, ca. 600 MPa, whereas for the $45^\circ/135^\circ$ and $60^\circ/120^\circ$ topologies values of 850 MPa and 700 MPa were achieved respectively. This means that plastic deformation is reached for the orientation $45^\circ/135^\circ$, since the maximum stress values obtained exceed the yield strength of CoCr alloy. For compression tests, Figs. 6 (a)-(c) also show that no significant differences in maximum stress values are observed for the different internal topologies analyzed.

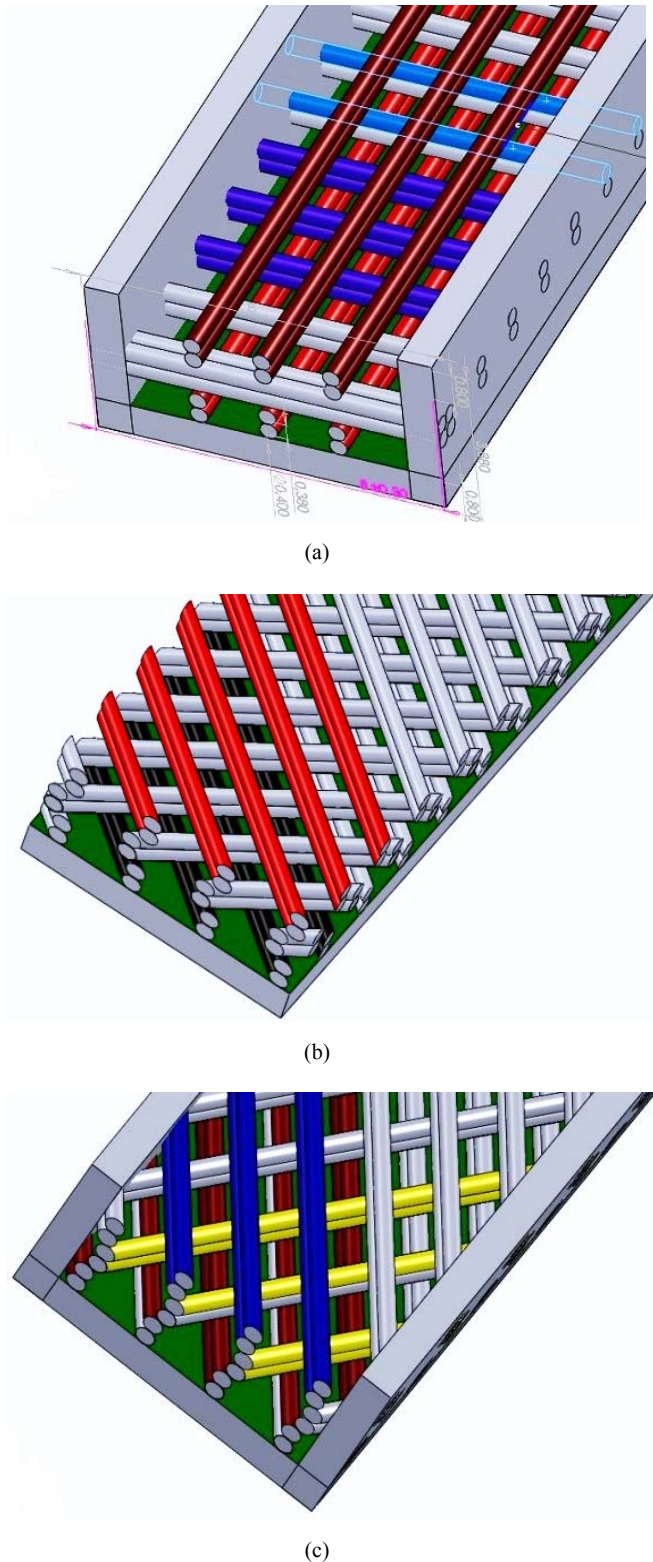
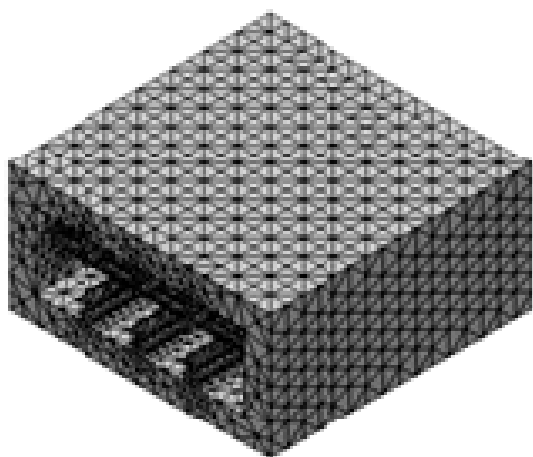
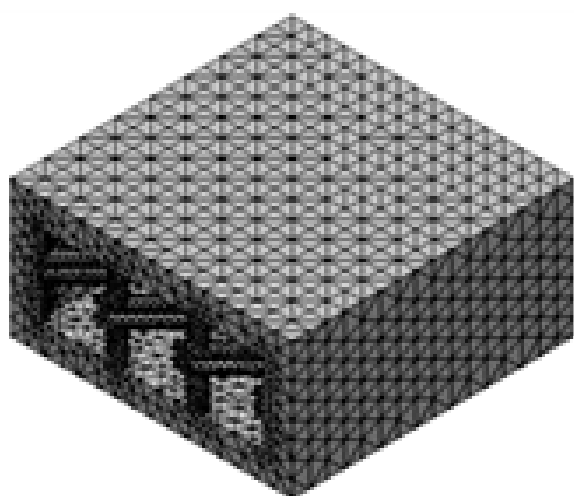


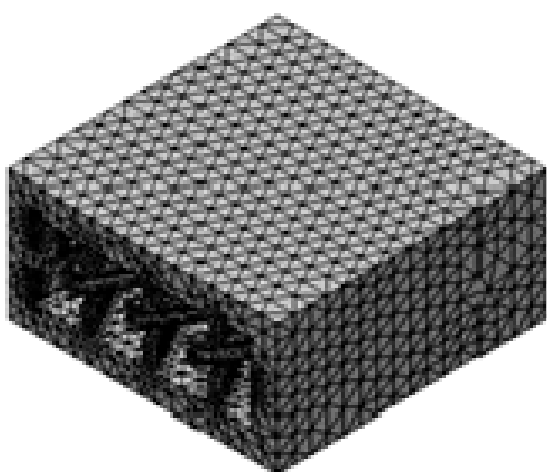
Fig. 1 3D CAD for (a) $0^\circ/90^\circ$, (b) $45^\circ/135^\circ$ and (c) $60^\circ/120^\circ$ internal topologies developed



(a)

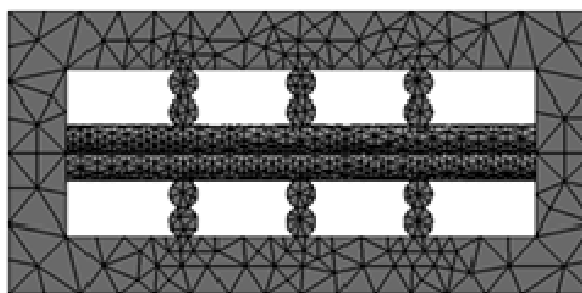


(b)

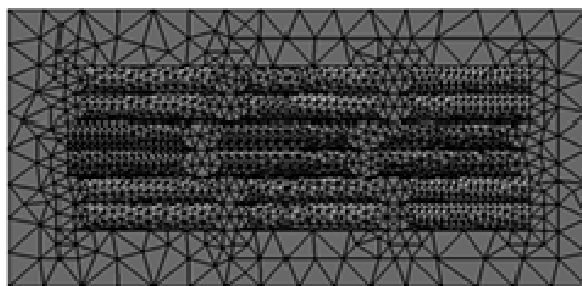


(c)

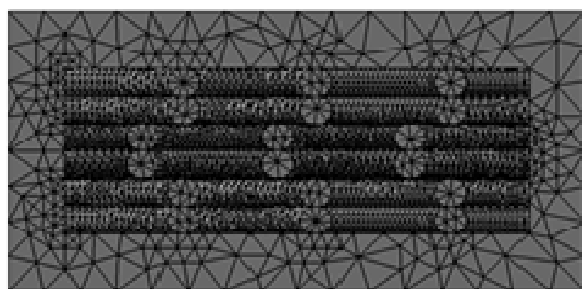
Fig. 2 3D finite element model for (a) 0°/90°, (b) 45°/135° and (c) 60°/120° internal topologies developed



(a)



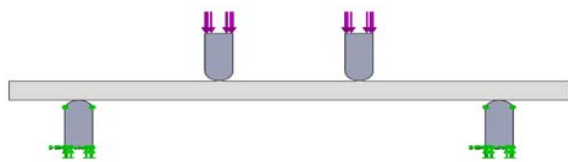
(b)



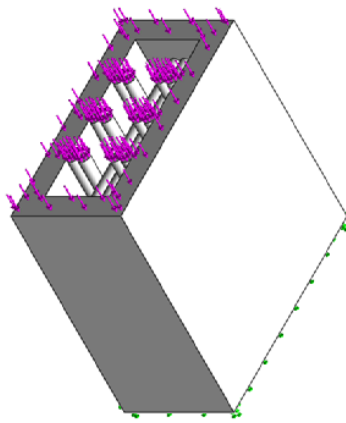
(c)

Fig. 3 Cross section of 3D finite element model for (a) 0°/90°, (b) 45°/135° and (c) 60°/120° internal topologies developed

The stress values reached at the coated box and the adjacent filaments of 0/90 internal topology are, however, greatest than those verified for the topologies 45/135 and 60/120. The lowest stress values, of the order of 500 MPa, are verified for the inner zone of test specimen corresponding to topology of 0/90 which corresponds to the filaments oriented at 0°. Regardless of inner filaments orientation, the value of the tensile strength of CoCr alloy was clearly exceeded reaching lower values for the 60°/120° topology.

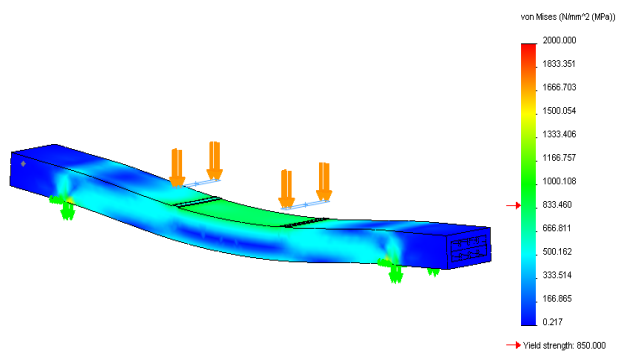


(a)

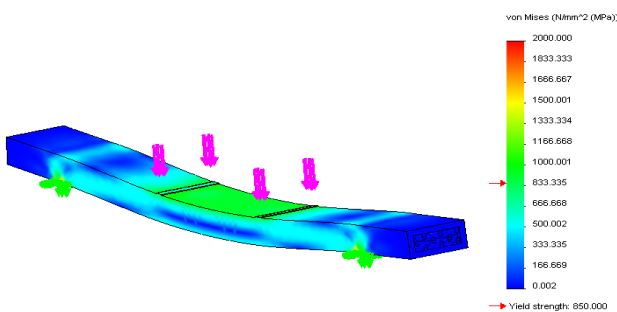


(b)

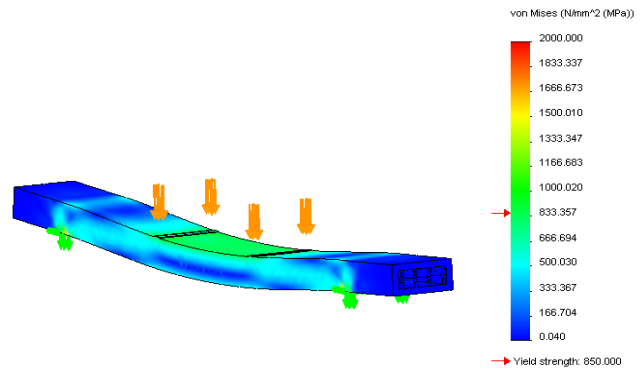
Fig. 4 Boundary and load conditions for the 3D CAD model developed: (a) bending and (b) compression tests



(a)

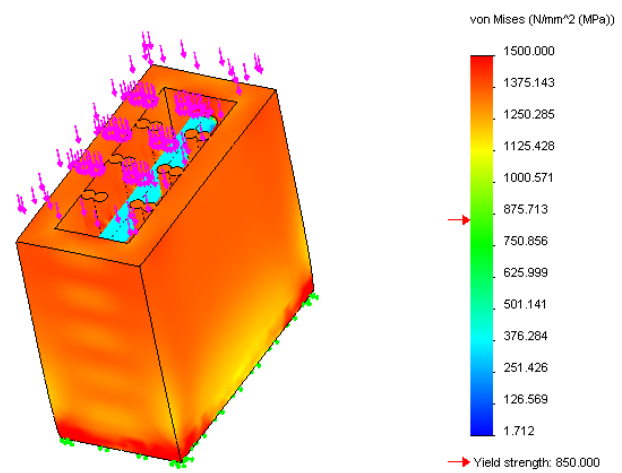


(b)

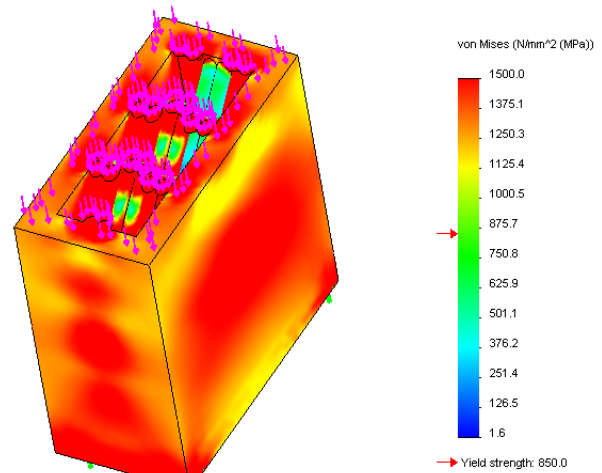


(c)

Fig. 5 FEA of three topologies developed when submitted to four point bending tests



(a)



(b)

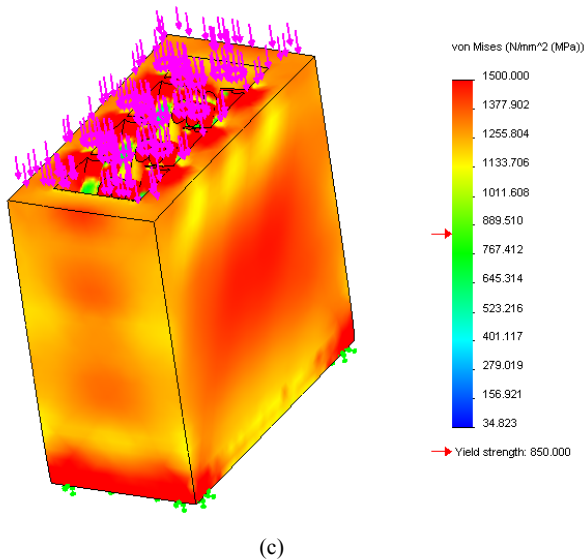


Fig. 6 FEA of three topologies developed when submitted to compression tests

IV. CONCLUSION

Bending and compression test specimens, coated with parallelepiped shell, were produced with three alternative internal topologies in terms of inner filaments orientation: $0^\circ/90^\circ$; $45^\circ/135^\circ$; and $60^\circ/120^\circ$. The internal topologies modeled in this work aimed at the production of components with a high degree of porosity compared to fully dense components, although not compromising its structural behavior and strength. The porosity obtained, regardless of the topology type, was similar for all specimens, with values between 70 and 80%. These values decreased with the addition of the casing near to theoretical values of 40%. Simulation results show that mechanical properties depend on the type and direction of the applied mechanical load. Specimens with porous internal geometry oriented $0^\circ/90^\circ$ seem to have a better mechanical behavior for bending test, while the topology $60^\circ/120^\circ$ seems to present a superior mechanical behavior when submitted to compression loads. These results require, however, experimental validation in order to optimize the ratio porosity vs. mechanical behavior, since differences between alternative internal topologies seem to be not relevant.

REFERENCES

- [1] J.-P. Kruth; M. Badrossamay; E.Yasa, J. Deckers, L. Thijs, J. Van Humbeeck, "Part and material properties in selective laser melting of metals," 16th International Symposium on Electromachining, ISEM XVI, 2010.
- [2] J.-P. Kruth, G. Levy, F. Klocke, T.H.C. Childs, "Consolidation phenomena in laser and powder-bed based layered manufacturing," CIRP Annals, vol. 56 (2), 2007, pp. 730-759.
- [3] E. Yasa, J. Deckers, J.-P. Kruth, M. Rombouts and J. Luyten, "Charpy impact testing of metallic selective laser melting parts," Virtual and Physical Prototyping, 5 (2), 2010, pp. 89-98.
- [4] I. Yadroitsev, L. Thivillon, Ph. Bertrand, I. Smurov, "Strategy of manufacturing components with designed internal structure by selective laser melting of metallic powder," Applied Surface Science, 254, 2007, pp. 980-983.
- [5] L. Hao, S. Dadbakhsh, O. Seaman, M. Felstead, "Selective laser melting of a stainless steel and hydroxyapatite composite for load-bearing implant development," Journal of Materials Processing Technology, 209, 2009, pp. 5793-5801.
- [6] M. Khan and P. Dickens, "Selective Laser Melting (SLM) of pure gold, Gold Bulletin, 43 (2), 2010, pp. 114-121.
- [7] B.-J. Joo, J.-H. Jang, J.-H. Lee, Y.-M. Son, Y.-H. Moon, "Selective laser melting of Fe-Ni-Cr layer on AISI H13 tool steel," Trans. Nonferrous Met. Soc. China, 19, 2009, pp. 921-924.
- [8] P. Fox, S. Pogson, C.J. Sutcliffe, E. Jones, "Interface interactions between porous titanium/tantalum coatings, produced by Selective Laser Melting (SLM), on a cobalt-chromium alloy," Surface & Coatings Technology, 202, 2008, pp. 5001-5007.
- [9] M. Domingos, D. Dinucci, S. Cometa, M. Alderighi, P. J. Bártolo and F. Chiellini, "Polycaprolactone scaffolds fabricated via bioextrusion for tissue engineering applications," International Journal of Biomaterials, 2009, pp. 1-9.